Research Article | Vol. 30, No. 15 / 18 Jul 2022 / Optics Express 26787
Optics EXPRESS

Amorphous silicon carbide high contrast gratings as highly efficient spectrally selective visible reflectors

HALEY C. BAUSER,[1] MORGAN D. FOLEY,[2] MEGAN E. PHELAN,[1] WILLIAM WEIGAND,[3] DAVID R. NEEDELL,[1] ZACHARY C. HOLMAN,[3] AND HARRY A. ATWATER[1,*]

[1]*Department of Applied Physics and Materials Science, California Institute of Technology, 1200 E California Blvd, Pasadena, CA 91125, USA*
[2]*Department of Physics, California Institute of Technology, 1200 E California Blvd, Pasadena, CA 91125, USA*
[3]*School of Electrical, Computer, and Energy Engineering, Arizona State University, Tempe, AZ 85287, USA*
[*]*haa@caltech.edu*

Abstract: We report spectrally selective visible wavelength reflectors using hydrogenated amorphous silicon carbide (a-SiC:H) as a high index contrast material. Beyond 610nm and through the near infrared spectrum, a-SiC:H exhibits very low loss and exhibits an wavelength averaged index of refraction of n = 3.1. Here we design, fabricate, and characterize such visible reflectors using a hexagonal array of a-SiC:H nanopillars as wavelength-selective mirrors with a stop-band of approximately 40 nm full-width at half maximum. The fabricated high contrast grating exhibits reflectivity R >94% at a resonance wavelength of 642nm with a single layer of a-SiC:H nanopillars. The resonance wavelength is tunable by adjusting the geometrical parameters of the a-SiC:H nanopillar array, and we observe a stop-band spectral center shift from 635 nm up to 642 nm. High contrast gratings formed from a-SiC:H nanopillars are a promising platform for various visible wavelength nanophotonics applications.

1. Introduction

The ability to manipulate light in the visible spectrum in high index, virtually lossless photonic systems is of great importance for many nanophotonics applications including photonic sensors, beam steering components for LIDAR, photonic integrated circuits, on-chip resonators, and meta-lenses [1–7]. Typical nanophotonic systems require high index materials in order to induce the required scattering phase and amplitude values [9]. One example includes photonic waveguides applications in sensing and local communication, where high index materials provide an increase in the local density of states [8–10]. At the same time, the high index material must also exhibit a near-zero extinction coefficient. Many state-of-the-art high index materials do not satisfy these two requirements, and exhibit either excessive absorption in visible spectrum (e.g., Si, a-Si) or an index of refraction that is too low (e.g., TiO2) [11,12]. While there are some III-V semiconducting materials that have a high index of refraction and near-zero extinction coefficient in the visible spectrum, such as GaP and AlSb, mass deployment of these materials in nanophotonic technologies is limited by technically challenging or costly deposition methods [13–15]. Here we introduce hydrogenated amorphous silicon carbide (a-SiC:H) as a high index material for photonic applications; a-SiC:H exhibits near-zero absorption at and beyond 600nm and maintains an index of refraction of approximately n = 3 beyond 800 nm [16,17]. Figure 1 shows the measured permittivity (n,k) data as a function of wavelength for 200nm to 1700nm.

To demonstrate the potential of a-SiC:H nanophotonic structures within the visible spectrum, we design and fabricate spectrally selective high-contrast grating reflectors. High contrast gratings

#456898 https://doi.org/10.1364/OE.456898
Journal © 2022 Received 6 Mar 2022; revised 28 Apr 2022; accepted 28 Apr 2022; published 11 Jul 2022

Optics EXPRESS

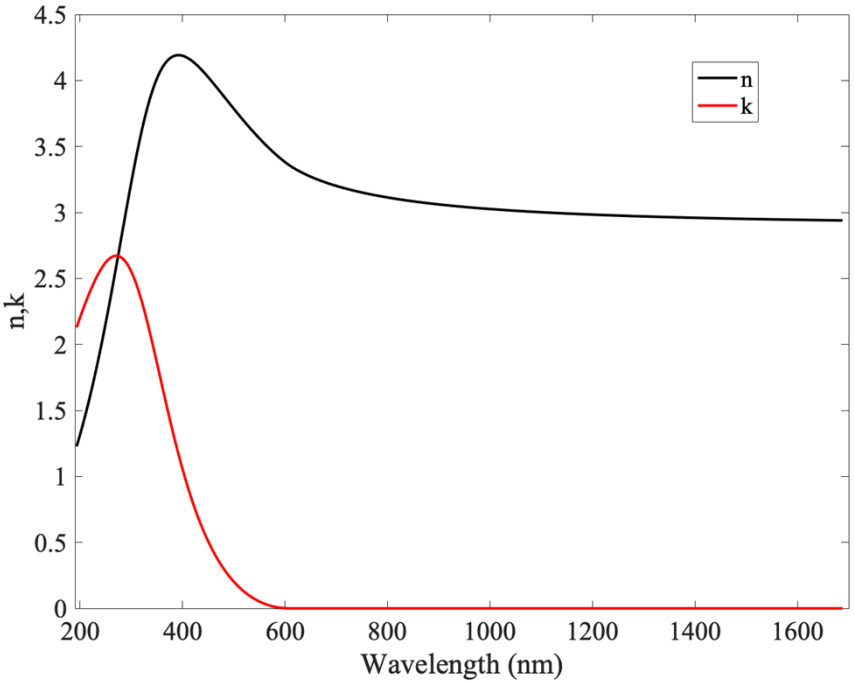

Fig. 1. Index of refraction and extinction coefficient of a-SiC:H measured via spectroscopic ellipsometry.

(HCGs) consist of a single layer of high index material patterned on a low index substrate. The application of HCGs as spectrally selective reflectors (e.g., stop-band reflectors) could provide the photonics communities with a simple single-layer alternative to Bragg filters. While Bragg filters can achieve near-unity reflectance, they are difficulty to fabricate over large areas, and the stop-band blue-shifts at increasing angles of incidence—limiting their use in applications which require isotropy (e.g., as mirror for photoluminescence emission or scattering for varying incident angle light sources [18,19]. HCGs are capable of achieving high reflectivity with a sharper reflection peak [8,20]. Periodic HCG reflectors can also be fabricated using nano-imprint lithography, opening the potential for scalability in mass manufacturing [21–23]. Furthermore, HCGs demonstrate high performance with a single layer of high index material, on the order of 1μm thickness, making them well-suited to applications requiring lightweight modules [8,9,20].

An understanding of the spectrally selective high reflectivity of HCGs can in part be derived from analytical Mie theory, in which the pillars act as Mie resonators creating interference in the transverse electric and magnetic modes of the incident light [20,24,25]. The incident light therefore couples to guided modes within the resonating array [9]. Given this mechanism, HCG reflectance patterns differ from Bragg filters (which rely upon constructive and destructive wave interference through many layers of alternating low/high index materials) by exhibiting a resonant peak, where modes are guided into the HCG substrates or any coverings for the HCG array [8]. By adjusting the physical parameters of the HCG array geometry (pitch, feature size, thickness), we can alter the guided modes' resonant wavelength, thereby tuning the peak reflectivity [8,9,14,20]. The overall thickness and spectral tunability of HCGs could enable such structures to technologically disrupt various photonic applications (e.g., metalenses, broadband spectral reflectors) [7,14,20].

Optics EXPRESS

2. Simulation results

To demonstrate the utility of a-SiC:H HCGs as spectrally selective reflectors, we design and fabricate a hexagonal nanopillar array optimized for a reflection peak at 635nm. We select 635nm as the peak center to match the spectral properties and extensive application of CdSe/CdS quantum dots in the photovoltaics, display, and lighting industries [26–29]. Such a spectrally selective HCG reflector is of particular use for photovoltaics applications in luminescent solar concentrators [25,30–32]. By integrating a HCG reflector in a tandem luminescent solar concentrator using CdSe/CdS QD luminophores, the overall module efficiency can be increased by over 4% [30,31]. For reflection peaks at or below 650nm, a-SiC:H is particularly well-suited given its lossless characteristics shown in Fig. 1—whereas many other HCG materials exhibit large parasitic extinction coefficients in this spectrum [12]. We adopt the hexagonal array structure to achieve narrower peaks with smaller sweeping angles than its square or rectangular array counterparts [31]. We use a quartz substrate for the a-SiC:H pillars given its low extinction coefficient, therefore yielding maximum reflectance of the a-SiC:H array.

We determine optimal physical parameters of the HCG array via Lumerical Finite Difference Time Domain (FDTD) simulations. We simulate a broadband (300–1100 nm) plane wave source and apply periodic boundary conditions to our HCG hexagonal unit cell to best approximate an infinite nanopillar array across many unit cells. We place monitors above the nanopillars and below the substrate to account for reflected and transmitted light, respectively. We measured the optical constants of the a-SiC:H layer via ellipsometry and employ experimental measured n,k values for a-SiC:H in our simulation. The quartz optical constants were derived from Maltison

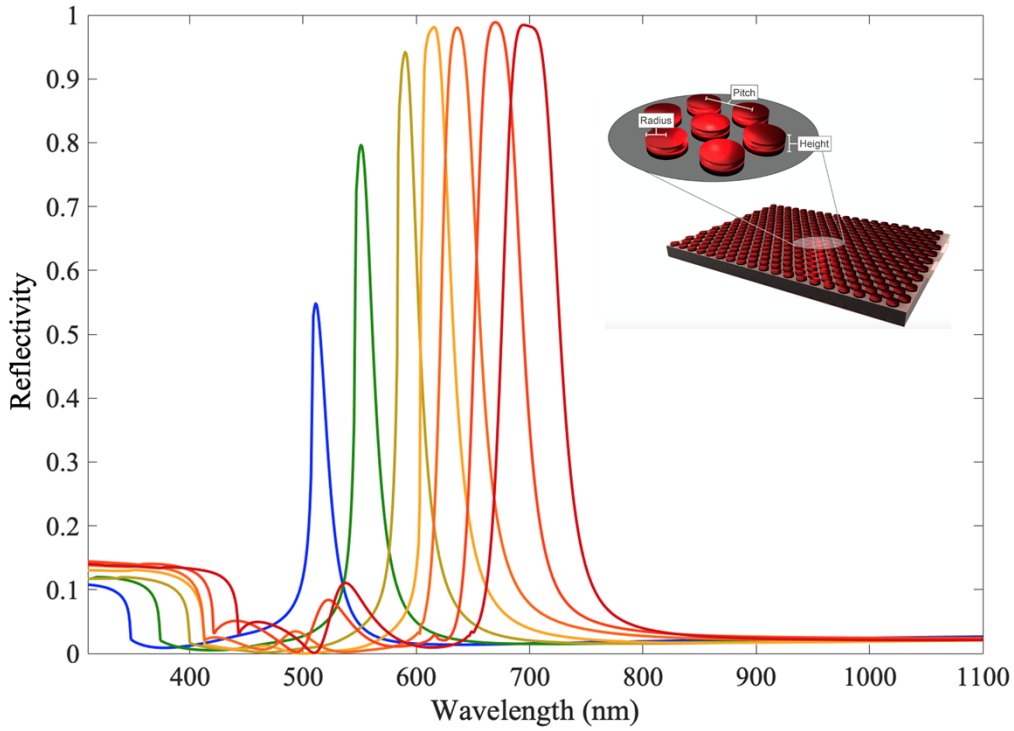

Fig. 2. Demonstration of how adjusting the geometric parameters of the high contrast grating reflector (pitch, radius, and thickness), shifts the resonance wavelength. By decreasing the geometric parameters, resonance can be tuned down to 500nm. By increasing the geometric parameters, we can observe resonance to the edge of the visible spectrum.

Optics EXPRESS

[33]. To fully resolve the optical modes of the array, we systematically varied the a-SiC:H nanopillar pitch, radius, and array thickness to optimize for the reflectance at 635 nm. Figure 2 shows the effect of varying the radius, pitch, and height on the spectrally selective reflector resonance peak. Generally, smaller nanopillar geometric features result in shorter wavelength resonances. Likewise, larger nanopillar features red-shifted the resonances. Increasing and decreasing the radius results in a reflection peak at a shorter and longer wavelength, respectively. Increasing the thickness generates a stronger peak, but if the thickness increases too much, a bi-modal reflection is observed. Lastly, increasing the pitch decreases the width of the reflection peak. These observed behaviors corresponded with prior work [30,31]. To corroborate these trends, the (SI) summarizes these trends for fabricated HCGs. Given our target reflectance spectrum, we determine the optimal pitch, pillar radius, and pillar thickness to be 475 nm, 125 nm, and 120 nm respectively. These parameters result in a simulated reflectivity of R = 97.8% reflectance at 635 nm, as illustrated in Fig. 3.

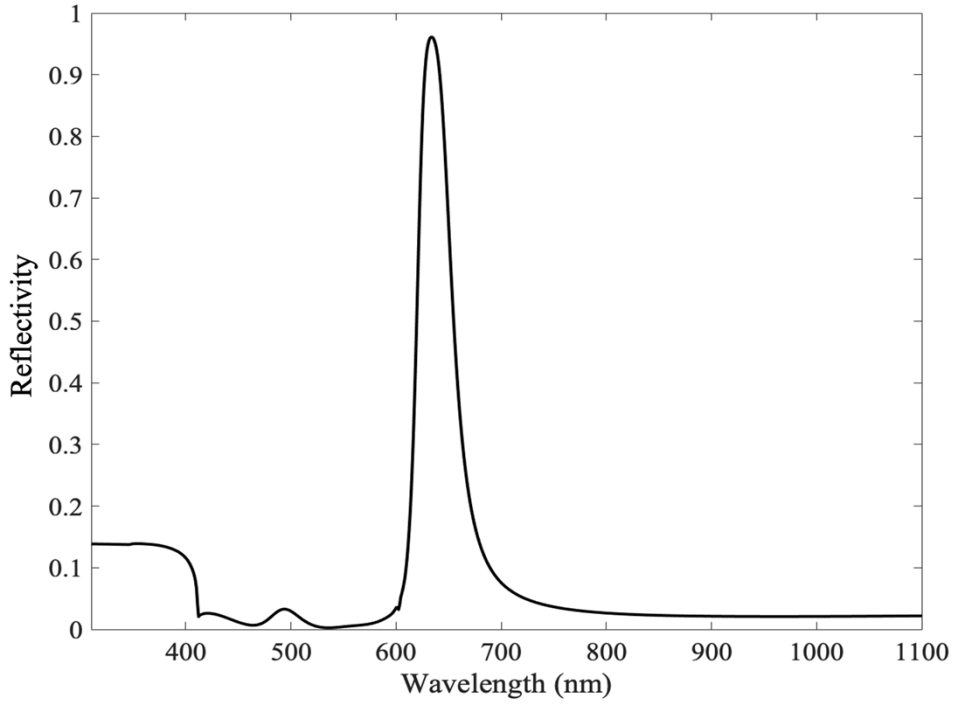

Fig. 3. Simulated a-SiC:H high contrast reflector with a reflectivity of 97.8% at 635nm.

3. Experimental results and discussion

Informed by these design parameters, we next fabricated hexagonal a-SiC:H nanopillar array HCGs via electron beam lithography. Figure 4 shows measured reflectance spectra for a-SiC:H HCGs with a maximum reflectance peak of approximately R = 94.4% at 642 nm, and R = 92% at 635 nm. We observe modest deviations in the resonance behavior of the fabricated HCGs compared to the simulation parameters. Through our imaging, we find the radius of the fabricated pillars to be, on average, consistent with the simulation optimum of 125 nm. However, the measured reflectance showed higher sensitivity to the a-SiC:H thickness than that seen in simulations. Previous studies corroborate our findings and suggest that when a HCG becomes too thick, multiple resonances appear [30,32] While simulations showed 120 nm to be the ideal

Optics EXPRESS

a-SiC:H layer thickness, we measured the fabricated thickness of the pillars to be 128 nm. Finally, we find nanopillar pitch to be the parameter with the largest disparity between simulations and experiments. Our fabricated HCG sample exhibits an average pitch of 455nm between the pillars, whereas our calculations indicated an optimum pitch of 475nm. We found that a higher fill fraction generally resulted in a higher reflectivity for fabricated HCG reflectors. A smaller pitch, and therefore higher fill fraction, can ultimately result in a sharper peak which can have a greater effect on the overall reflectivity as errors accumulate on the substrate [30,31]. Electromagnetic simulations employed periodic boundary conditions with identical unit cells of the HCG, that are not realistic in full pattern fabrication [34]. While integrating across the area of the fabricated HCG reflector includes imperfections on the HCG surface contributing to the variation in the optimal geometric parameters, opting for the full area measurement demonstrates a more realistic reflector performance [20,34–36].

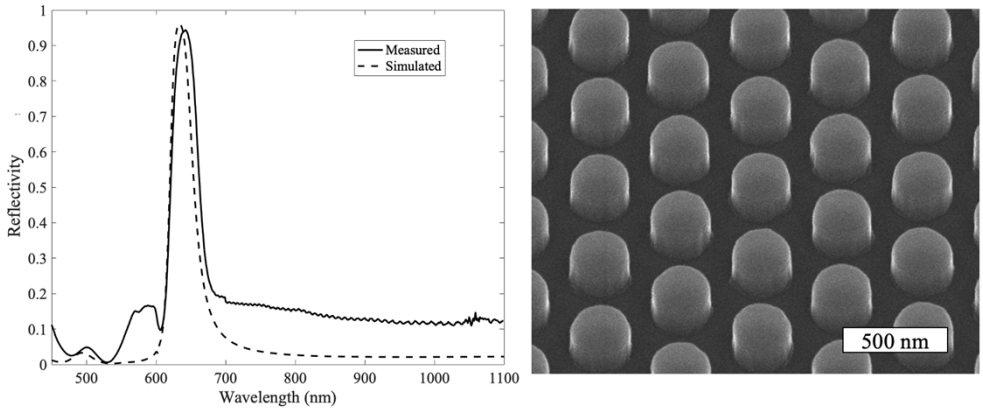

Fig. 4. The left shows the reflection profile of a fabricated a-SiC:H spectrally selective reflector overlayed with the simulated reflection peak. The right is a SEM image of the hexagonal nanopillar array a-SiC:H reflector. The SEM image includes a thin layer of sputtered Cr as a conduction layer.

4. Conclusions

We have designed, and fabricated a-SiC:H spectrally selective high-contrast gratings suitable for high reflectivity with a narrow stop-band, matched to semiconductor quantum dots with photoluminescence emission centered at 635nm. Further, calculations indicate high reflectivity resonance peaks across the visible spectrum using spectrally-selective HCGs comprised of a hexagonal array of a-SiC:H nanopillars. While our experimentally validated example comprises a single stop-band of interest, this study illustrates the material and design potential for many low-loss high index applications in the photonics community.

5. Methods

We deposit the a-SiC:H layer by PECVD onto quartz substrates using previously reported methods [16]. The a-SiC:H was deposited under a pressure of 4.3 mbar and temperature of 250 degrees Celsius. The gas flow is a mixture of silane, methane, and hydrogen. The methane flow ratio (defined as the methane mass flow divided by the sum of the methane and silane mass flow) was held at 75% which has been shown to maintain a lower extinction coefficient at shorter wavelengths. The hydrogen flow was set to 1600 sccm to induce a higher index of refraction while maintaining a near-zero extinction coefficient in our region of interest. The index of

Optics EXPRESS

refraction and extinction coefficients in Fig. 1 were measured via ellipsometry, which was fit with a sensitivity on the order of 10^{-6}.We spin-coated negative tone electron beam resist layers (MaN-2403) onto the a-SiC:H—at 3000 rpm for 30 seconds. We next spin-coat a solution of 99% poly(4-stryenesulfonic acid) and 1% Triton X-100 surfactant directly onto the resist as a water-soluble sacrificial layer, which we deposit 10 nm of Au onto via thermal evaporation [20]. This Au layer acts as a conductive agent to prevent charging over the insulating and dielectric materials of the nanopillar array. We pattern the array with a Raith 5200 electron beam writer (electron source set at 100 kV, beam current at 5 nA, and dose at 340μC/cm^2). After inscribing the pattern, we remove the Au and sacrificial layer by a one minute water bath. We develop the array in a base developer (MF-319) for one minute. We etch the array for 90 seconds using an Oxford ICP-RIE with a pseudo-Bosch SF_6/C_4F_8 process—forward power of 1500W and a 32W ICP power with a gas flow of 22 sccm of SF_6 and 30 sccm of C_4F_8. Finally, we remove the remaining resist via O_2 plasma—20 minutes at a pressure of 20 mTorr, power of 80W, and flow of 20 sccm.

We measured the reflectance of a-SiC:H hexagonal array HCGs via a supercontinuum laser light source coupled with a monochromator to provide a narrow spot size (~10 μm) around each wavelength. Reflection measurements were taken between 450 nm and 1100 nm at normal incidence. Non polarizing beam splitters were used to direct the reflected beam to a Si photodiode. A NIST-calibrated Specular Reflectance Ag mirror (STAN-SSH-NIST) was used to normalize raw reflectivity. The spot-size of the reflectance measurements integrates across the entire 700μmx700μm area of the fabricated HCG.

Funding. Office of Science (DE-SC0019140); Space Solar Power Project; National Science Foundation (EEC-1041895).

Disclosures. The authors declare no conflicts of interest

Data availability. Data underlying the results presented in this paper are not publicly available at this time but may be obtained from the authors upon reasonable request.

Supplemental document. See Supplement 1 for supporting content.

References

1. W. Peng and H. Wu, "Flexible Stretchable Photonic Sensors Based on Modulation of Light Transmission," Adv. Opt. Mater. **7**(12), 1900329 (2019).
2. P. Parimi, W. T. Lu, P. Vodo, and S. Sridhar, "Imaging by flat lens using negative refraction," Nature **426**(6965), 404 (2003).
3. P. Camayad-Munoz, C. Ballew, G. Roberts, and A. Faraon, "Multifunctional volumetric meta-optics for color and polarization image sensors," Optica **7**(4), 280–283 (2020).
4. J. Xu, M. Cua, E. H. Zhou, Y. Horie, A. Faraon, and C. Yang, "Wide-angular-range and high-resolution beam steering by a metasurface-coupled phase array.",," Opt. Lett. **43**(21), 5255–5258 (2018).
5. F. Kish, R. Nagarajan, D. Welch, P. Evans, J. Rossi, J. Pleumeekers, A. Dentai, M. Kato, S. Corzine, R. Muthiah, M. Ziari, R. Schneider, N. Reffle, T. Butrie, D. Lambert, M. Missey, V. Lal, M. Fisher, S. Murthy, R. Salvatore, S. Demars, A. James, and C. Joyner, "From visible light-emitting diodes to large-scale III-V photonic integrated circuits," Proc. IEEE **101**(10), 2255–2270 (2013).
6. X. Lu, Q. Li, D. A. Westly, G. Moille, A. Singh, V. Anant, and K. Srinivasan, "Chip-integrated visible-telecom entangled photon pair source for quantum communication," Nat. Phys. **15**(4), 373–381 (2019).
7. S. Tan, F. Yang, V. Boominathan, A. Veeraraghavan, and G. V. Naik, "3D imagine using extreme dispersion in optical metasurfaces," ACS Photonics **8**(5), 1421–1429 (2021).
8. C. Chang-Hansain and W. Yang, "High-contrast gratings for integrated optoelectronics," Adv. Opt. Photon. **4**(3), 379–440 (2012).
9. Y. Ding and R. Magnusson, "Band gaps and leaky-wave effects in resonant photonic-crystal waveguides," Opt. Express **15**(2), 680–694 (2007).
10. L. Novotny and B. Hecht, *Principles of Nano-Optics*. Cambridge University Press, (2006).
11. Y. Wu, W. Yang, Y. Fan, Q. Song, and S. Xiao, "TiO_2 metasurfaces: From visible planar photonics to photochemistry," Sci. Adv. **5**(11), 11 (2019).
12. D. E. Aspnes and A. A. Stunda, "Dielectric functions and optical parameters of Si, Ge, GaP, GaAs, GaSb, InP, InAs, and InSb from 1.5 to 6.0 eV," Phys. Rev. Lett. **64**(2), 192–195 (1990).
13. H. Emmer, C. T. Chen, R. Saive, D. Friedrich, Y. Horie, A. Arbabi, A. Faraon, and H. A. Atwater, "Fabrication of Single Crystal Gallium Phosphide Thin Films on Glass," Sci. Rep. **7**(1), 4643 (2017).

Optics EXPRESS

14. H. C. Bauser, D. R. Needell, and H. A. Atwater, "AlSb as a material for high index contrast nanophotonics," Opt. Mater. Express **11**(5), 1334–1342 (2021).
15. D. G. Baranov, D. A. Zuev, S. I. Lepeshov, O. V. Kotov, A. E. Krasnok, A. B. Evlyukhin, and B. N. Chichkov, "All-dielectric nanophotonics: the quest for better materials and fabrication techniques," Optica **4**(7), 814–825 (2017).
16. M. Boccard and Z. C. Holman, "Amorphous silicon carbide passivating layers for crystalline-silicon-based heterojunction solar cells," J. Appl. Phys. **118**(6), 065704 (2015).
17. H. C. Bauser, C. R. Bukowsky, M. Phelan, W. Weigand, D. R. Needell, Z. C. Holman, and H. A. Atwater, "Photonic crystal waveguides for >90% light trapping efficiency in luminescent solar concentrators," ACS Photonics **7**(8), 2122–2131 (2020).
18. J. W. Leem, X. Guan, and J. S. Yu, "Tunable distributed Bragg reflectors with wide-angle and broadband high-reflectivity using nanoporous/dense titanium dioxide film stacks for visible wavelength applications," Opt. Express 22(15), 18519–18526 (2014).
19. P. Baumeister, *Optical Coating Technology*; SPIE Press: Bellingham, Washington, U.S.A., (2004).
20. R. C. Ng, J. C. Garcia, J. R. Greer, and K. T. Fountaine, "Polarization-Independent, Narrowband, Near-IR Spectral Filters via Guided Mode Resonances in Ultrathin a-Si Nanopillar Arrays," ACS Photonics **6**(2), 265–271 (2019).
21. D. K. Oh, T. Lee, B. Ko, T. Badlow, J. G. Ok, and J. Rho, "Nanoimprint lithography for high-throughput fabrication of metasurfaces," Front. Optoelectron. **14**(2), 229–251 (2021).
22. C. A. Dirdal, G. U. Jensen, H. Angelskar, P. C. V. Thran, J. Gjessing, and D. A. Ordung, "Towards high-throughput large-area metalens fabrication using UV-nanoimprint lithography and Bosch deep reactive ion etching," Opt. Express **28**(10), 15542–15561 (2020).
23. V. J. Einck, M. Torfeh, A. McClung, D. E. Jung, M. Mansouree, A. Arbabi, and J. J. Watkins, "Scalable Nanoimprint Lithography Process for Manufacturing Visible Metasurfaces Composed of High Aspect Ratio TiO2 Meta-Atoms," ACS Photonics **8**(8), 2400–2409 (2021).
24. P. P. Iyer, N. A. Butakov, and J. A. Schuller, "Reconfigurable semiconductor phased-array metasurfaces," ACS Photonics **2**(8), 1077–1084 (2015).
25. T. Wriedt, "Mie Theory: A Review," In: W. Herget and T. Wriedt eds., *The Mie Theory Springer Series in Optical Sciences Berlin*, Germany, vol 169 2012.
26. D. A. Hanifi, N. D. Bronstein, B. A. Koscher, Z. Nett, J. K. Swabeck, K. Takano, A. S. Schwartzberg, L. Maserati, K. Vandewal, Y. Van De Burgt, A. Salleo, and A. P. Alivisatos, "Redefining Near-Unity Luminescence in Quantum Dots with Photothermal Threshold Quantum Yield," Science **363**(6432), 1199–1202 (2019).
27. D. R. Needell, O. Ilic, C. R. Bukowsky, Z. Nett, L. Xu, J. He, H. Bauser, B. G. Lee, J. F. Geisz, R. G. Nuzzo, A. P. Alivisatos, and H. A. Atwater, "Design Criteria for Micro-Optical Tandem Luminescent Solar Concentrators," IEEE J. Photovoltaics **8**(6), 1560–1567 (2018).
28. T. Kim, K. Cho, E.K. Lee, S.J. Lee, J. Chae, J.W. Kim, D.H. Kim, J. Kwon, G. Amaratunga, S.Y. Lee, B. L. Choi, Y. Kuk, J.M. Kim, and K. Kim, "Full-colour quantum dot displays fabricated by transfer printing," Nat. Photonics **5**(3), 176–182 (2011).
29. B. Li, M. Lu, J. Feng, J. Zhang, P.M. Smowton, J. I. Sohn, I Park, H. Zhong, and B. Hou, "Colloidal quantum dot hybrids: and emerging class of materials for ambient lighting," J. Mater. Chem. C **8**(31), 10676–10695 (2020).
30. H. Bauser, D.R. Needell, C.R. Bukowsky, O. Ilic, Z. Nett, B.G. Lee, J.F. Geisz, A.P. Alivisatos, and H. A. Atwater, "Metasurfaces as wavelength selective mirrors in tandem luminescent solar concentrators," *PVSC 45th Conference Proceedings* (2018).
31. S. Darbe and H. A. Atwater, "Resonant dielectric high-contrast gratings as spectrum splitting optical elements for ultrahigh efficiency (>50%) photovoltaics," *2015 PVSC, 42nd Conference Proceedings* (2015).
32. D. R. Needell, C. R. Bukowsky, S. Darbe, H. Bauser, O. Ilic, and H. A. Atwater, "Spectrally matched quantum dot photoluminescent in GaAs-Si tandem luminescent solar concentrators," IEEE J. Photovoltaics **9**(2), 397–401 (2019).
33. I. H. Maltison, "Interspecimen comparison of the refractive index of fused silica," J. Opt. Soc. Am. **55**(10), 1205–1208 (1965).
34. Y. Yao, H. Liu, and W. Wu, "Fabricaiton of high-contrast gratings for a parallel spectrum splitting dispersive element in a concentrated photovoltaic system," J. Vacuum Sci. Technol. B **32**(6), 06FG04 (2014).
35. N. Unno, "Thermal roll-to-roll imprinted nanogratings on plastic film," J. Vacuum Sci. Technol. B **32**(6), 06FG03 (2014).
36. B. Hogan, S. P. Hegarty, L. Lewis, J. Romero-Vivas, T. J. Ochalski, and G. Huyet, "Realization of high-contrast gratings operating at 10(m," Opt. Lett. **41**(21), 5130–5133 (2016).